

Modelling the distribution, sustainability and diapause emergence timing of the copepod *Calanus finmarchicus* in the Labrador Sea

D. P. TITTENSOR,¹ B. DEYOUNG^{1,*} AND
C. L. TANG²

¹Department of Physics and Physical Oceanography, Memorial University of Newfoundland, St. John's, Newfoundland A1B 3X7, Canada

²Bedford Institute of Oceanography, Dartmouth, Nova Scotia, Canada

ABSTRACT

It is now recognized that *Calanus finmarchicus*, the dominant copepod zooplankter of the North Atlantic, has most of its biomass in the open ocean. While the Labrador Sea does contain a large population of *Calanus finmarchicus*, the importance of possible connections with the rest of the North Atlantic are not understood. Although there are few wintertime observations, sufficient data exist to model the role of the circulation, temperature and food supply on population dynamics. This study couples a biological model of *Calanus finmarchicus* with a physical oceanographic model of the Labrador Sea, using chlorophyll data derived from observations by the satellite-borne SeaWiFS (Sea-viewing Wide Field-of-view Sensor) as a proxy food supply for the numerical copepods. We produce a large-scale, comprehensive picture of the spatial distribution of *Calanus finmarchicus* in the Labrador Sea, along with an exploration of the timing of diapause and an examination of population sustainability. We are able to simulate reasonably well the temporal and spatial patterns of *Calanus finmarchicus* in the Labrador Sea. During a year long model run, the population has a single generation over most of the Labrador Sea, with a final diapausing population about 50% the size of the initial for the parameters used in these simulations. A latitudinally dependent diapause emergence scheme

with early emergence to the south of Newfoundland provides the best fit to data. A change of 0.5°C in the temperature field can cause significant changes in the population abundance in a single year, due to changes in *Calanus finmarchicus* growth rates.

Key words: *Calanus finmarchicus*, climate impacts, diapause, Labrador Sea, population model, SeaWiFS

INTRODUCTION

Calanus finmarchicus is the dominant zooplankter in terms of biomass throughout much of the North Atlantic (Planque, 1997), including the Labrador Sea (Kielhorn, 1952; Huntley *et al.*, 1983; Head *et al.*, 2000). Near surface *C. finmarchicus* distributions in this area have been quantified for almost 50 yr by means of the Continuous Plankton Recorder (CPR) survey (Planque, 1997). The distribution of *C. finmarchicus* as derived from CPR data shows considerable spatial heterogeneity, with three regions of high abundance – the southern part of the Labrador Sea and waters between south-west Greenland and Newfoundland, the waters off the west coast of Norway, and the slope water off the Scotian Shelf – which are separated by areas of lower concentration (Planque, 1997). CPR data, however, are dependent upon ships of opportunity, which rarely venture into the mid- and northern Labrador Sea, especially when it is ice-covered during the winter, so long-term, detailed data sets for these locations are not available. In addition, *C. finmarchicus* are often located at depth in diapause during the winter months (Hirche, 1996), and as the CPR comprises tow data from the top 10 m, CPR data only represent surface population features and activity. The need for a comprehensive depiction of seasonal distributions throughout the entire Labrador Sea is thus clear.

The primary population centres for *C. finmarchicus* in the North Atlantic (Head *et al.*, 2001; Heath *et al.*, 2001) each occupy one of the primary gyres of this region: the Norwegian Sea gyre and the Labrador/Irminger Sea gyre (Fig. 1). While there is clearly the

*Correspondence. e-mail: bdeyoung@physics.mun.ca

Received 25 October 2002

Revised version accepted 15 June 2003

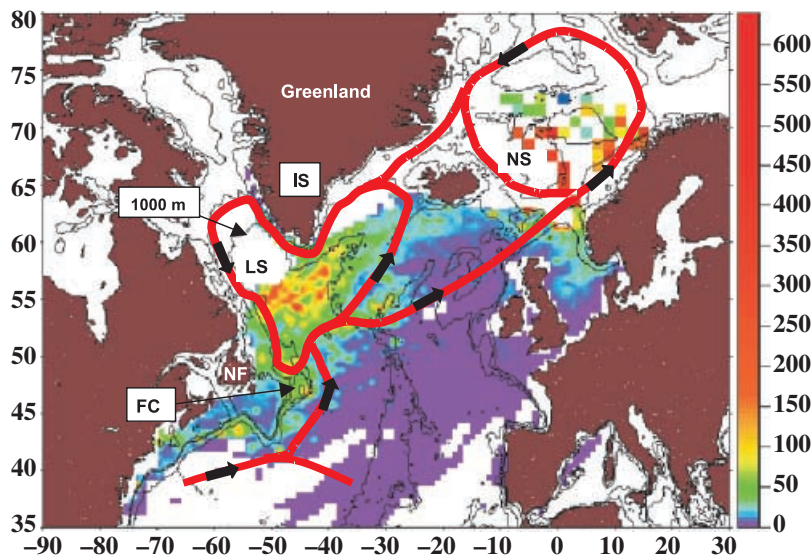


Figure 1. The mean abundance of *Calanus finmarchicus* (number/3 m⁻³) stages CV–CVI in the North Atlantic based primarily on CPR data during 1950–99. From Heath *et al.* (2001), with a schematic diagram of the gyre system within the North Atlantic overlaid. Note the relationship between the population maxima of *Calanus finmarchicus* and the gyres. LS, Labrador Sea; IS, Irminger Sea; NF, Newfoundland; FC, Flemish Cap. The 1000-m isobath is marked at the upper left.

potential for exchange between these gyres, it is not yet known how important the exchange might be for the separate populations or the maintenance of *Calanus* in the North Atlantic. The time scale for circulation around these gyres is as long as, or longer, than the annual life cycle of the organism (Dickson *et al.*, 1988). It is quite likely that the large-scale circulation plays some role in the basin-scale population dynamics of this copepod. We proposed to model *C. finmarchicus* in the Labrador Sea to determine the influence of temperature, food supply and circulation on the regional population dynamics of this organism.

Modelling the population structure of an organism barely visible to the eye across a region greater than a million square kilometres, several kilometres deep, is a serious challenge. Our approach is focused on the large-scale patterns and results, given the limited data on the organism in this region, the present limitations of the biological and physical models, and the uncertainty in the parameterization and initialization of the models, in particular the biological model (Carlotti *et al.*, 2000).

We use data from prior experimental and modelling studies of *C. finmarchicus* to parameterize and calibrate a biological model that is then coupled with three-dimensional velocity and temperature fields derived from a physical circulation model. A spatially explicit, bimonthly chlorophyll data set derived from remotely sensed SeaWiFS (Sea-viewing Wide Field-of-view Sensor) observations is used as a food proxy. Model output over the course of an annual cycle is then compared with existing data sets from the Labrador Sea. Particular attention is paid to the

timing of emergence from diapause and how this affects the fit of the model to data. The question of self-sustainability for a population in the Labrador Sea with no advection of individuals into the region is also addressed.

We begin with the biological model, based on that of Trela *et al.* (2003), a linearly distributed weight-based model, which provides a reasonable balance between the minimization of computational demands (an important consideration for insertion within a three-dimensional system) and the provision of an accurate representation of population dynamics. Life history features such as diapause, non-feeding stages, and stage-specific moulting weights have been added to the model. The extensive literature on modelling *C. finmarchicus* provides a benchmark with which to validate accuracy.

The circulation field is from the three-dimensional, seasonally averaged, diagnostic model of Yao *et al.* (2000), a coupled system of models consisting of a multicategory ice model and a regionally adapted Princeton Ocean Model (Blumberg and Mellor, 1987; Mellor, 1996). Use of a diagnostic model allows for reproduction of essential features in current velocity while maintaining the system at a level of complexity, which simplifies the analysis of results. We use the phytoplankton concentration as an index for the food supply in order to model the growth of *C. finmarchicus* without making any assumption that they are primarily herbivorous (Mauchline, 1998). Phytoplankton density is derived from SeaWiFS images (Hooker *et al.*, 1992; Hooker and McLain, 2000), within the box locations described by Petrie and Mason (2000).

MODEL STRUCTURE AND DATA INTEGRATION

Biological model

Population modelling has been extensively utilized as a tool to analyse zooplankton population dynamics, with approaches being divided into several categories, including stage and weight structured models, matrix models, cohort models, individual-based models (e.g. Carlotti and Wolf, 1998) and Lagrangian ensemble models (e.g. Woods and Barkmann, 1993). Zooplankton models may further be integrated within community and ecosystem models. More recently, spatially explicit models have been created to examine regional population dynamics (Heath *et al.*, 1997; Lynch *et al.*, 1998; Miller *et al.*, 1998). Carlotti *et al.* (2000) provide an exhaustive reference of zooplankton modelling techniques.

Here we apply a weight-based model (Trela *et al.*, unpublished data) that represents the integrated weight of individuals within each class by a linear distribution rather than a single variable; this distribution is specifically considered when calculating weight-dependent growth within each class. The individual bioenergetics of the model closely follow Bryant *et al.* (1997). The distribution within each weight class changes in relation to individual growth, which itself depends upon temperature and food availability. The primary benefit of the linear distribution within each weight class is the substantial reduction in numerical diffusion. Periods of positive growth can lead to a transfer of individuals to the class above, while negative net growth eventually results in starvation mortality. For brevity, only basic model equations and changes from the original specification for the purposes of this study are mentioned; a complete model description is available in Trela *et al.* (unpublished data).

Eight classes are present within the model (see Table 1), each of which represents one or more stage in the life history of *C. finmarchicus*. This was judged

to be the minimum number necessary to represent the important behavioural and physical differences between stages, while still maintaining computational feasibility for inclusion within a three-dimensional model system. The inclusion of separate classes for immature females and diapausing individuals allows for a more accurate representation of sexual development and seasonal behaviour (Lynch *et al.*, 1998). The class structure is based upon physiological similarities between stages that are incorporated within each particular class (Mauchline, 1998). Only stages that have similar metabolic processes are grouped together; thus the non-feeding egg and nauplii stages (Carlotti and Radach, 1996; Carlotti and Wolf, 1998) are contained within one class, as are N3–N6 and CI–CIV. The model encompasses differing growth rates for individuals of the same class but different weights due to the functional representation of bioenergetics and the linear intra-class distribution.

Each class is enclosed by a lower weight boundary, w_i , and an upper weight boundary, w_{i+1} . The weights are structural only, and do not include lipid stores. Moulting weights for each stage are difficult to determine, as there is significant variation regionally (Carlotti *et al.*, 1993), between individuals (McLaren, 1986), and as a function of temperature.

The weight-based categories provide a reasonable representation of key stages, while allowing for individual variability with the linear weight distribution within each class. The weight of newly laid eggs is set to $0.3 \mu\text{g C}$ (Carlotti and Wolf, 1998). N1 and N2 stages do not eat, and as their development is purely temperature-dependent (Carlotti and Radach, 1996) there are no moulting weights for early nauplii, simply a weight loss from metabolic processes. Progress through these stages is determined by ambient temperature. Moulting weights to copepodite classes are determined by the literature values for the North-west Atlantic compiled by Carlotti *et al.* (1993). As there is a large variation in the range of observations, we use the mid-point between the high-weight value and the low-weight value in each case. Maturation weight for females is considered to be the adult weight plus an additional 20%, a value similar to that in Carlotti and Radach (1996) for moulting at 8°C ; the maximum mature female weight in the model still lies within the range of combined literature weights reported by Carlotti *et al.* (1993). Inclusion of a separate class for mature females forces a lag between maturation to adulthood and egg laying; this is to simulate the necessity of building up an adequate lipid supply prior to reproduction. The moulting weights are presented in Table 2.

Table 1. Classes within the *Calanus finmarchicus* model.

Class no.	Stage(s)
1	Egg, N1, N2
2	N3–N6
3	CI–CIV
4	CV
5	CV (diapause)
6	Immature female
7	Mature female
8	Male

Table 2. Moulting weights to class, all in $\mu\text{g C}$.

Class	Moulting weight to class
3 (CI–CIV)	3.8
4 (CV)	108.0
6 (immature female)/8 (male)	217.0
7 mature female	260.0

Individuals within class i are weight distributed following the linear functions of Trela *et al.* (2003). These linear functions represent changes in intra-class weight distribution, thus allowing for a range of weights for individuals within each class. This approach provides greater fidelity when modelling growth, and minimizes the numerical diffusion common to this approach while at the same time permitting greater numerical efficiency. The number of individuals in class i is N_i , and the summed weight of individuals W_i . The time rate of change of individuals in class i can be represented in differential equation form as follows:

$$\frac{dN_i}{dt} = T_{i-1}^N - T_i^N - \delta_i N_i, \quad (1)$$

$$T_i^N = [A(w_{i+1})]^+ n(w_{i+1}), \quad (2)$$

where T_i^N is transfer to class $i + 1$ from class i , δ_i mortality, $A(w_{i+1})$ net assimilation of individuals at weight w_{i+1} , and $n(w_{i+1})$ the number of individuals at weight w_{i+1} , the upper weight boundary of class i , that is the weight at which the transition to the next weight class would occur. Within this manuscript, $[x]^+$ denotes the function $f(x)$ where $f(x) = \max[x, 0]$; thus transfer of individuals to the next class occurs only when the net assimilation within the class is positive. The representation for the time rate of change of weight in class i is similar:

$$\frac{dW_i}{dt} = T_{i-1}^w - T_i^w + [G_i]^+ - \delta W_i, \quad (3)$$

$$T_i^w = T_i^N w_{i+1}, \quad (4)$$

where $[G_i]^+$ is the net assimilation within class i .

Growth for eggs and individuals in stages N1 and N2 (class 1) follows the Bêlehrádek function (Corkett *et al.*, 1986), with development time for stage i in days given as:

$$D(T) = a_i(T - \beta)^\alpha, \quad (5)$$

where T is the ambient temperature, $\alpha = -2.05$, and $\beta = -9.11^\circ\text{C}$. The values of the parameter a_i follow Lynch *et al.* (1998), and are summed for the three stages in class 1, giving a final value of 1564.

As they do not feed, eggs, N1 and N2 individuals lose body weight equivalent to their metabolic costs at each time step. Diapausing individuals (class 5) are assumed not to feed or grow (Lynch *et al.*, 1998) and energy expenditure is assumed to be insignificant, as metabolism is greatly reduced during diapause (Hirche, 1996; Ingvarsdottir *et al.*, 1999). Adult males (class 8) are considered to feed and grow, with an upper weight cap equal to that of mature females (class 7); although they play no further part in the model after reaching adulthood, they are tracked simply to retain an accurate measure of *C. finmarchicus* biomass. The sex ratio for individuals maturing to adulthood is set to 0.5, a reasonable assumption although there is evidence that the sex ratio does at times differ from 0.5 (Irigoiien *et al.*, 2000).

Mature females do not grow, and are assumed to invest all net assimilation into egg production. The number of eggs produced by the population at each time-step is:

$$\beta = [G_7]^+ / w_1 \quad (6)$$

The individual food uptake rate U and basal metabolic cost M are:

$$U = aw^b \frac{P}{c + P} Q_{10}^{\left(\frac{T - T_{\text{ref}}}{10^\circ\text{C}}\right)}, \quad (7)$$

$$M = kw^g Q_{10}^{\left(\frac{T - T_{\text{ref}}}{10^\circ\text{C}}\right)}, \quad (8)$$

where a is the maximum uptake rate coefficient, b the maximum uptake exponent, c the food half-saturation concentration, P the phytoplankton concentration (in mg C m^{-3}), Q_{10} the temperature quotient, T_{ref} the reference temperature, k the basal costs coefficient, and g the basal costs exponent. Most of the parameters are held at a fixed value (Table 3), with the exception of the maximum uptake rate coefficient, a , which has a latitudinal dependency derived from matching one-dimensional model runs to data at two separate locations, one in the Labrador Sea and another to the south (more on these runs later).

The net assimilation rate A is calculated by subtracting the basal metabolic cost M from the assimilated uptake εU (where ε is the absorption efficiency); growth is thus dependent upon both ambient temperature and food availability.

Mortality for each class, δ_i , is composed of two components: background mortality and starvation mortality. Background mortality takes a constant value of 5% per day for all classes except diapausing individuals, which have a value 10 times smaller at 0.5% per day. Should starvation occur (i.e. net growth

Table 3. Parameters used within the *Calanus finmarchicus* model.

Parameter	Symbol	Units	Value	Source
Maximum uptake rate coefficient	a	$\text{mg C}^{(1-b)} \text{ day}^{-1}$	0.0828 at 40°N 0.13 at 57.38°N Interpolated between these two locations. Held constant north of 57.38°N	Tittensor (2002)
Maximum uptake rate exponent	b	–	0.7	Carlotti and Radach (1996)
Food half saturation concentration	c	mg C m^{-3}	25	Trela <i>et al.</i> (2003)
Basal costs coefficient	k	$\text{mg C}^{(1-g)} \text{ day}^{-1}$	0.0116	Trela <i>et al.</i> (2003)
Diapause entry factor	σ	–	0.5	Fixed
Diapause exit timing	dt	days	Varies between model runs	Fixed
Basal costs exponent	g	–	0.65	Trela <i>et al.</i> (2003)
Temperature quotient	Q_{10}	–	2.0	Trela <i>et al.</i> (2003)
Reference temperature of Q_{10}	T_{ref}	°C	10	Trela <i>et al.</i> (2003)
Absorption efficiency minus SDA	ε	–	0.6	Trela <i>et al.</i> (2003)
Mortality, non-diapausing classes	δ	day^{-1}	0.05	Fixed
Mortality, diapausing class	δ_d	day^{-1}	0.005	Fixed

is negative), then the weight of organisms within a class is reduced proportionally, until the mean weight of individuals approaches the lower boundary of the class, at which point starvation mortality occurs:

$$\delta_s = -\gamma_i/w_i, \quad (9)$$

where δ_s represents starvation mortality, and γ_i per capita net growth rate within class i . Mortality was parameterized by running the biological model in a one-dimensional form at two locations for which population data was available (Tittensor, 2002).

Diapausing individuals are considered to be CVs (Hirche, 1996); no other classes in the model can enter or exit diapause. The diapause function utilizes a timing parameter, dt , in days. Beginning on day $dt + 1$, and continuing until day $dt + 30$, the proportion of (at-depth) CVs exiting diapause at each time-step is equal to $(t - dt)/30$. For the rest of the year, individuals do not exit diapause. Thus all individuals exit diapause within a 30-day span, with most individuals exiting in the early part of this period. This short time-span for ascent of the population from diapause matches Kielhorn's (1952) Bravo data.

The proportion of (surface CV) individuals entering diapause on each particular day is set to σ , the diapause entry parameter. If the value of σ is low, then most CV individuals of each new generation will remain at the surface and moult to adult; if it is high, individuals have a greater chance of entering diapause. As individuals that moult to CV in the same time-step may not enter diapause simultaneously, zooplankton of differing weights can enter diapause. Note that CVs of the G0 generation cannot re-enter diapause.

Given that most of the Labrador Sea region appears only to have one generation or, if a second generation does appear, it is insignificant in terms of regional production (Kielhorn, 1952; Head *et al.*, 2000), the value of σ is set to 0.5. This allows for a second generation, but it is unlikely and very much dependent upon development rates. Unless individuals develop extremely quickly (due to high temperatures and/or food availability) a second generation would be small, if indeed it appears at all. This fits well with available data on *C. finmarchicus* in the region (Kielhorn, 1952; Huntley *et al.*, 1983).

Table 3 lists the various parameters that are used in the *C. finmarchicus* model.

Physical model

We require a physical model of the Labrador Sea in order to determine the influence of the circulation on the mean population structure of *C. finmarchicus* in this region, and the potential role of diapause in population dynamics (Backhaus *et al.*, 1994). The Labrador Sea spans a region of 10^6 km^2 , with a maximum depth of 3000 m. The cyclonic circulation (Fig. 1) is driven by wind forcing over the Labrador Sea, regional freshwater inputs, and convection associated with winter cooling (Lazier and Wright, 1993). Sea ice formation and melting also plays a significant role (Yao *et al.*, 2000). The Labrador Sea is of major interest oceanographically for its deep convection processes (Clarke and Gascard, 1983; Marshall *et al.*, 1998).

Output from the model of Yao *et al.* (2000), a sigma-coordinate Princeton Ocean Model (Blumberg

and Mellor, 1987; Mellor, 1996) with an embedded second-order turbulence closure submodel and a coupled multicategory ice model, is integrated with the *C. finmarchicus* model and provides seasonally averaged flow and temperature fields for the Labrador Sea. The model has a free surface and uses time splitting for the external mode. Horizontal diffusion follows sigma surfaces and uses a Smagorinsky diffusivity. The above references contain all the model equations in full detail.

Monthly climatological data from the National Centers for Environmental Prediction (NCEP)/National Center for Atmospheric Research (NCAR) reanalysis (Kalnay *et al.*, 1996), obtained from the National Oceanic and Atmospheric Administration Climate Diagnostics Center as monthly averages, are used for atmospheric forcing. Air temperature at 2 m, specific humidity at 2 m, precipitation and cloudiness are averaged over the period from 1974 to 1996 to produce a monthly climatology. Wind at 10-m and 6-h intervals, also from the NCEP/NCAR reanalysis, is used to derive wind stress and the values are then used in the calculation of heat flux. The drag coefficient is calculated as a function of wind speed and air-sea temperature differences (Smith, 1988). Initial ocean temperature and salinity are obtained from an objective analysis of data (Tang and Wang, 1996).

Atmospheric data are bilinearly interpolated to fit the model grid of $1/5^\circ$ latitude \times $1/6^\circ$ longitude. The model equations are solved using a spherical coordinate system, with a domain ranging from 40 to 66° N and 40 to 66° W; note, however, that this is neither precisely the same as the region of interest nor the same grid size as the output used within the coupled model system. The sixteen vertical sigma levels are as follows: 0, -0.02, -0.04, -0.08, -0.17, -0.25, -0.33, -0.42, -0.50, -0.58, -0.67, -0.75, -0.83, -0.92, -0.96 and -1.00. Prescribed transports occur at open boundaries (cf. Yao *et al.* (2000)). The velocity and temperature fields are output matrices that are used in the coupled-model system.

SeaWiFS data

Although *C. finmarchicus* may not be solely herbivorous (Mauchline, 1998), we will use phytoplankton as an index for food supply. Within the Labrador Sea the timing of ascent from diapause and coincidence with the initiation of the spring bloom seems to be important for population survival (Head *et al.*, 2000). The modelling of phytoplankton as a food source therefore takes on considerable importance.

Chlorophyll data from the SeaWiFS satellite-mounted sensor (Hooker *et al.*, 1992; Hooker and

McLain, 2000) are used for the modelled region. These values are then used as a proxy of food availability for *C. finmarchicus*. SeaWiFS is a second-generation remote colour sensor, capable of detecting eight separate bands between 402 and 885 nm. SeaWiFS captures colour images that are calibrated, analysed and processed in order to extract information about chlorophyll *a* concentrations and other biogeochemical properties (Hooker *et al.*, 1992; McClain *et al.*, 1992; Aiken *et al.*, 1995; Hooker and McLain, 2000). Data from the Labrador Sea region have been collated (Petrie and Mason, 2000; P. Pepin & G. Harrison, personal communication) and analysed for a number of locations (Table 4).

Mean chlorophyll within each location (Table 4) is provided in bimonthly form from 1998 to 2000, and is then further compiled over this 3-yr period in order to provide a composite annual picture (in 2-week intervals) of chlorophyll concentration. If for any 2-week period no data exists in any year of the 3-yr span, it is linearly interpolated from the surrounding values. Chlorophyll values are converted to carbon concentration (the units for food uptake in the biological model) using a C : Chl ratio of 50 (Trela, 1996; Head *et al.*, 2000). Phytoplankton concentrate is assumed to be constant over the mixed layer, a reasonable assumption if vertical mixing is strong enough to cause a uniform phytoplankton distribution down to the base of the mixed layer (Mann and Lazier, 1996), which is obviously dependent upon the climatology of the region in question (Smith and Dobson, 1984), but seems reasonable in a mid-to-high latitude region such as the Labrador Sea. In each of the SeaWiFS data locations (Table 4), the spring bloom (for the purposes of the modelled system) is defined to be the largest two

Table 4. SeaWiFS data regions included in the coupled-model system (Petrie and Mason, 2000; P. Pepin, personal communication; G. Harrison, personal communication).

Area	Latitude ($^\circ$ N)	Longitude ($^\circ$ W)
Avalon channel	46–48	51.5–53
Bravo	56.63–58.13	50.42–53.17
Green St Pierre	45.33–46.33	54–56
Hamilton Bank	53.5–54.5	54–56
Hudson Strait	60.51–61.40	62.72–64.55
Labrador Basin	53.5–54.5	42.5–43.5
Labrador Shelf	56.91–57.81	59.55–61.20
Southeast Flemish Cap	45–47	42–44
South-east Shoal	44–46	50–52
St Anthony Basin	50–52	53–55
West Greenland	61–62	50–52

consecutive peaks in the annual signal. As the boxes do not cover the entire model region, we interpolate the data to provide chlorophyll over the model domain. We use an inverse distance weighting function to generate bi-monthly maps of chlorophyll (Fig. 2).

In using the SeaWiFS data, we are assuming that the phytoplankton can be used as an index for the available food for *C. finmarchicus*, which seems reasonable (Mauchline, 1998). The coupling between the phytoplankton and *C. finmarchicus* is unidirectional, i.e. we ignore feedback from grazing pressure upon phytoplankton population density. There is no explicit alternative food supply, such as microzooplankton, in this model.

The spring bloom is in general later at higher latitudes, which fits with the Sverdrup critical depth hypothesis (Siegel *et al.*, 2002). The SeaWiFS chlorophyll concentrations are towards the lower end of those measured in the Labrador Sea by Head *et al.* (2000), but within the range of *in situ* observations. Uncompiled data from the SeaWiFS locations (no spatial or temporal averaging) show a considerable variance in values, with a maximum in some cases greater than twice that measured by Head *et al.* (2000). Within the model system, the uptake rate parameter a is tuned to provide a growth rate that matches well to the literature within the region (Kielhorn, 1952; Anderson, 1990).

Model coupling

Over the annual population cycle, we expect the circulation to strongly influence the distribution of the vertically migratory copepod, as will changes in the temperature with position, both in the vertical and the horizontal. Surface circulation patterns can differ significantly from those at depth, and thus may combine with *C. finmarchicus* behavioural patterns (especially emergence from, and entrance into, diapause) to determine population distributions (Backhaus *et al.*, 1994; Slagstad and Tande, 1996). Vertical and horizontal temperature gradients in the Labrador Sea may also influence population dynamics as growth and development are temperature-dependent, both in the model and in the ocean (Harris *et al.*, 2000).

The velocity and temperature output fields from Yao *et al.* (2000), originally in sigma-coordinates, are linearly interpolated to 19 standard depths (0, 20, 40, 60, 80, 100, 120, 140, 160, 180, 200, 300, 400, 500, 600, 700, 800, 900 and 1000 metres) at each grid location. In addition, the grid size of the three-dimensional system (originally $1/5^\circ$ latitude by $1/6^\circ$ longitude in the physical model) is reduced by a factor of four. These simplifications are necessary to reduce

the complexity of the coupled model system to a computationally manageable size. The model domain is $44\text{--}66^\circ\text{N}$ and $40\text{--}66^\circ\text{W}$. The velocity and temperature fields from the physical model are provided in seasonally averaged form: winter (January, February, March), spring (April, May, June), summer (July, August, September) and autumn (October, November, December).

The distribution of individuals in the horizontal plane within each 'grid box' in the model (each of which is centred on a grid point) is assumed to be homogenous. When individuals are advected at each time-step, the entire distribution is relocated according to the velocity field; thus, the percentage of individuals moved to a new location corresponds to the overlap between the new location of the distribution and each bordering grid box.

Diffusive processes are included as a normally distributed random walk function, as in eqn 10, and applied to the distribution of individuals within each grid box after advective processes have occurred.

$$R\sqrt{K_H\Delta t} \quad (10)$$

where R is a normally distributed random number, with $R \in [-1, 1]$, K_H the diffusion coefficient, set to a value of $10 \text{ m}^2 \text{ s}^{-1}$, and Δt the size of the time step.

The time-step of the biological model is 1 day; this is low enough to prevent individuals from progressing more than one stage per time-step within the conditions present in the modelled system. In order to prevent advective instabilities the physical model flow fields advect individuals every one-quarter of a day; this limits numerical dispersion to an acceptably low level, given the relative sizes of the current velocity and time-step. The boundary conditions are as follows: outward fluxes at the model boundaries are calculated following transport values derived from the physical model; any individuals that exit the area do not return. Inward flux of individuals at all model boundaries is set to zero. Seasonal changeover for transport, temperature, and mixed-layer depth in the three-dimensional model system occurs on 1 January (winter), 1 April (spring), 1 July (summer), and 1 October (autumn). *Calanus finmarchicus* is displaced by the modelled velocity fields, grows in relation to temperature and phytoplankton density, and follows an annual cycle (beginning on the first of January) that includes regionally dependent diapause entrance and emergence. A level 4.5 Runge-Kutta scheme (ode45) is used to solve the biological differential equations in Matlab (Mathworks, Inc., Natick, MA, USA).

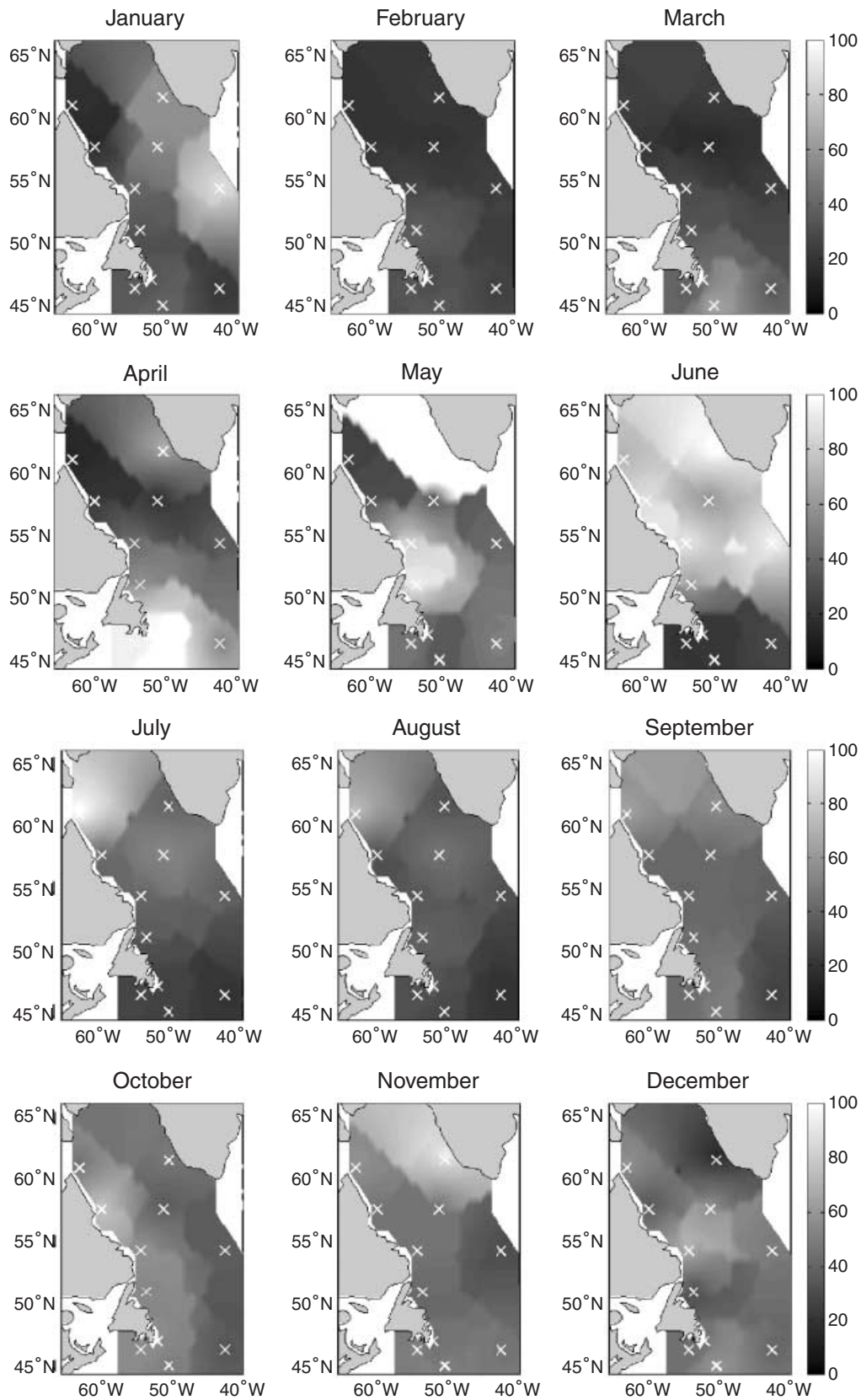


Figure 2. Interpolated phytoplankton density map for the model region. All values are in mg C m^{-3} . The white xs represent the centre of the SeaWiFS derived boxes.

Initial conditions

There are only a few primary sources of data for *C. finmarchicus* in the Labrador Sea. Kielhorn (1952) examined the planktonic ecology at Ocean Weather Station Bravo (OWS-B, $56^{\circ}30'N$, $51^{\circ}00'W$, roughly in the centre of the Labrador Sea) during the course of a full year (1950/51). These data reveal that diapause emergence occurs in April/May, with a G1 copepodite population maximum occurring in July/August. Around 10 yr later, the International Commission for the North-west Atlantic Fisheries conducted a series of cruises between April and July 1963 along transects within the Labrador Sea [ICNAF (International Commission for the North-west Atlantic Fisheries), 1963]. The *C. finmarchicus* data were summarized by Matthews (1968), with particular detail on the average stage of development at each location during the cruises:

- April, 1963. At most locations, adults were the mean stage of development. There were scattered CI–CIII present. Development was near-uniform across the survey region.
- June, 1963. Within all locations, the mean development stage was CI–CIII.
- July, 1963. The mean stage ranged from CI–CV, with the coast of Greenland being CI–CIII, and the central Labrador Sea CIV–CV. Development therefore appeared to be fastest in the central Labrador Sea.

All locations showed near-equivalence in April (suggesting that emergence from diapause had only recently occurred), with developmental differences becoming more pronounced on later cruises. There are substantial differences between Matthew's and Kielhorn's data – emergence is earlier and growth appears to be faster (if it is assumed that the maximum number of G1 copepodites consist of early stages, which is reasonable due to the cumulative effect of mortality on each stage) in the ICNAF survey.

Anderson (1990) examined a region around the Flemish Cap ($47^{\circ}N$, $45^{\circ}W$) during 1979–81. In April, the population was dominated by adults, but CI–CIVs were present by May. Individuals appeared to have reached CV by late June.

Planque (1997) examined over 30 yr of CPR data (1958–92) for *C. finmarchicus* CVs and adults, and

compiled the data into monthly log-abundance figures. A number of trends are observable from these data. There is a population to the south and east of Newfoundland that emerges from diapause much earlier than the rest of the region, with individuals present at the surface from November, and a high concentration appearing in February. For areas north of Newfoundland, individuals begin to appear at the surface in March or April, with high abundances from April to September.

Head *et al.* (2000) undertook a number of transect surveys in May–June of 1997, from around $42^{\circ}N$ to $64^{\circ}N$. CI–CIII individuals were (numerically) dominant in most of the northern region, with adults more abundant in the central and southern areas. Spring bloom conditions were late/post-bloom in the north, bloom conditions at the mid-latitudes, and early bloom in the south-east, and these conditions seemed consistent with those of the ICNAF surveys. Head *et al.* (2000) suggested that early blooms were common in the north and east, perhaps linked to the ice-melt. The hypothesis was put forward that the maturation of G0 females and development of the G1 generation was linked to the spring bloom, such that the G1 generation was more advanced in the north during the period surveyed due to the earlier bloom; differences in water temperature would then tend to speed up development and growth in southern regions.

The depth of diapause for *Calanus* varies around the North Atlantic but appears to range from 300 to 500 m (Miller *et al.*, 1991) down to 1000 m or deeper in the Faroe–Shetland Channel (Heath and Jónasdóttir, 1999; Heath *et al.*, 2000). There have been no observations of diapausing depth in the Labrador Sea, but 1000 m is considered to provide an adequate depth for the model. Individuals diapause at the deepest possible depth down to a maximum of 1000 m. The model results are not strongly sensitive to the choice of this depth as there is little stratification below 500 m (Clarke and Gascard, 1983). Upon emergence from diapause, they rise into the mixed layer. The mixed layer depth is defined to be the depth at which the temperature differs from the surface value by greater than $0.1^{\circ}C$. Individuals spread homogeneously within the mixed layer. Should individuals be advected to a new location in which they encounter subsurface topography, they rise to the deepest water at the new location.

The literature on *Calanus* in the North-west Atlantic suggests two hypotheses that can be discerned regarding emergence from diapause in the North-west Atlantic. It is also possible that each is correct, but for

different periods, and that the mechanisms by which diapause takes place has changed over time.

Hypothesis 1 – The latitudinal diapause hypothesis: Kielhorn (1952) indicates that emergence from diapause at Bravo (56°30'N) occurs in April/May, while Anderson (1990) presents data that would suggest emergence from diapause at Flemish Cap (47°N) to occur, by back-calculation from peak-spawning data, around the middle of March. From Planque (1997), emergence south of Newfoundland appears to be still earlier. Emergence from diapause is thus latitudinally dependent, being earlier in the south and later in the north.

Hypothesis 2 – The bi-latitudinal diapause hypothesis: from Matthews (1968) and Miller *et al.* (1991), it would appear that emergence from diapause occurs at roughly the same time over the entire region (most likely March), except to the south and east of Newfoundland where emergence appears to be earlier (Planque, 1997). Any differences that arise in population development may be due to different growth rates caused by the timing of the spring bloom and the temperature of the water (Head *et al.*, 2000).

Model runs

We set the biological parameters in the model by first running it in one-dimensional form at a few locations where we have the most complete population time series. With these model runs, we were able to reproduce the annual cycle of the observed population at a fixed location and maintain the final population numbers to within about 15% of the initial starting numbers. Figure 3 shows an example one-dimensional model run. We found that the population abundance was optimized in the middle of the Labrador Sea when the *Calanus* exited diapause about 30–60 days prior to the start of the spring bloom. By comparing the results for setting up the model in the middle of the Labrador Sea to match the Kielhorn (1952) time series, or near the Flemish Cap to match the time series of Anderson (1990), we set the value for the maximum uptake rate coefficient, a , to be linearly dependent on latitude. We tuned the final vertical one-dimensional runs using the seasonal temperature field taken from Yao *et al.*'s (2000) physical model.

Model run 1 utilizes latitudinally dependent emergence derived from the one-dimensional model at

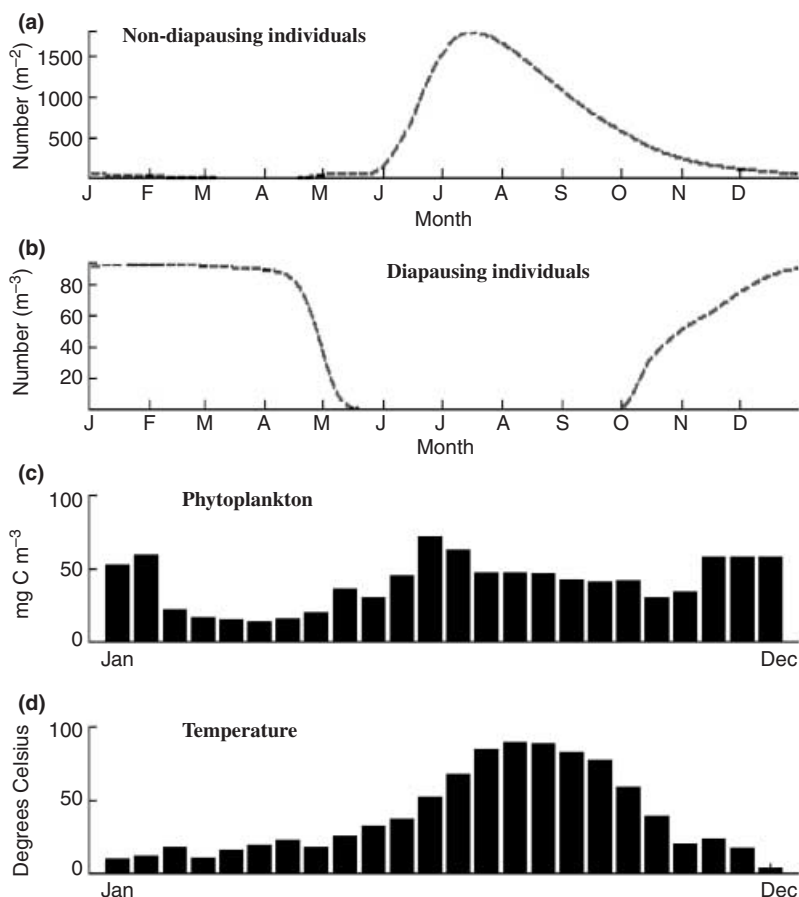


Figure 3. Population development of selected *Calanus finmarchicus* showing individuals total numbers not in diapause (a) and in diapause (b), phytoplankton density (c), and temperature (d) over an annual cycle during a one-dimensional run at the centre of the Bravo SeaWiFS box (57.38°N, 51.80°W). Temperature field is derived from interpolated 1969 Weather Station data (Lazier, 1980).

several locations (Tittensor, 2002) as follows; in mid-March at and below 47°N, in early May at and north of 57°N, and linearly interpolated at points in between. This diapause emergence timing fits the observations of Kielhorn (1952) and Anderson (1990).

Model run 2 has individuals emerging simultaneously over the entire region beginning in mid-March. This is done to represent the simplest possible spatial model of diapause, rather than having a separate scheme for those individuals to the south of Newfoundland.

Model run 3 applies the bi-latitudinal emergence model, matching to the data of Matthews (1968), with emergence occurring simultaneously in the Labrador Sea, while being much earlier to the south of Newfoundland. All individuals north of 50°N emerge in mid-March, while individuals to the south of 50°N emerge in mid-January, as observed in Planque (1997).

RESULTS

All the model runs begin with uniform distributions of organisms at 1000 m (Fig. 4a), with 100 diapausing

individuals at each location in which the water is of at least this depth. All model runs are for 1 yr. Statistics for the different runs are presented in Table 5. We plot the results from the runs showing the monthly averaged surface CV and adult concentrations. The patterns of concentration are clearly strongly influenced by the circulation patterns with production of a new generation, a population maximum in the central Labrador Sea region, and a final population of diapausing individuals that is significantly different from the initial all clearly visible. Model run 1 clearly shows the influence of advection, the final diapausing population displaying significant heterogeneity, and individuals on shelf and slope regions (Fig. 4b). Emergence from diapause can be seen to occur in the southern regions first, and spread northwards (Fig. 5). In addition, once females produce eggs, the differences between surface current patterns and those at depth becomes readily apparent, as the surface individuals are spread over a much larger region than occupied by the diapausing individuals. The final population in Fig. 4(b) shows that circulation and population productivity yield quite complex population patterns.

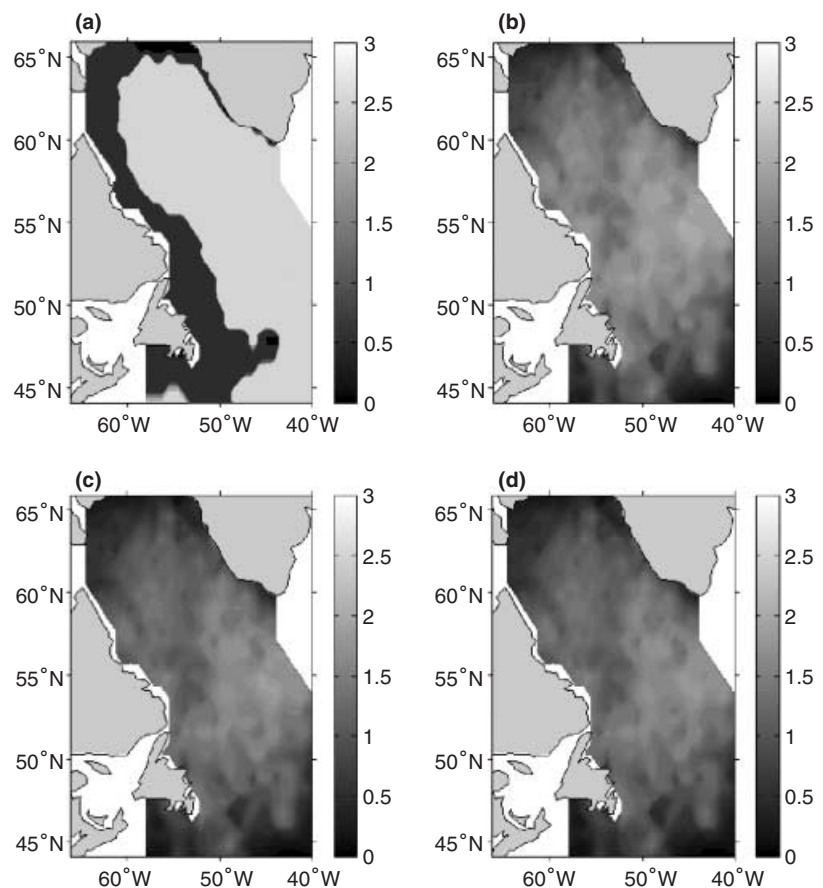
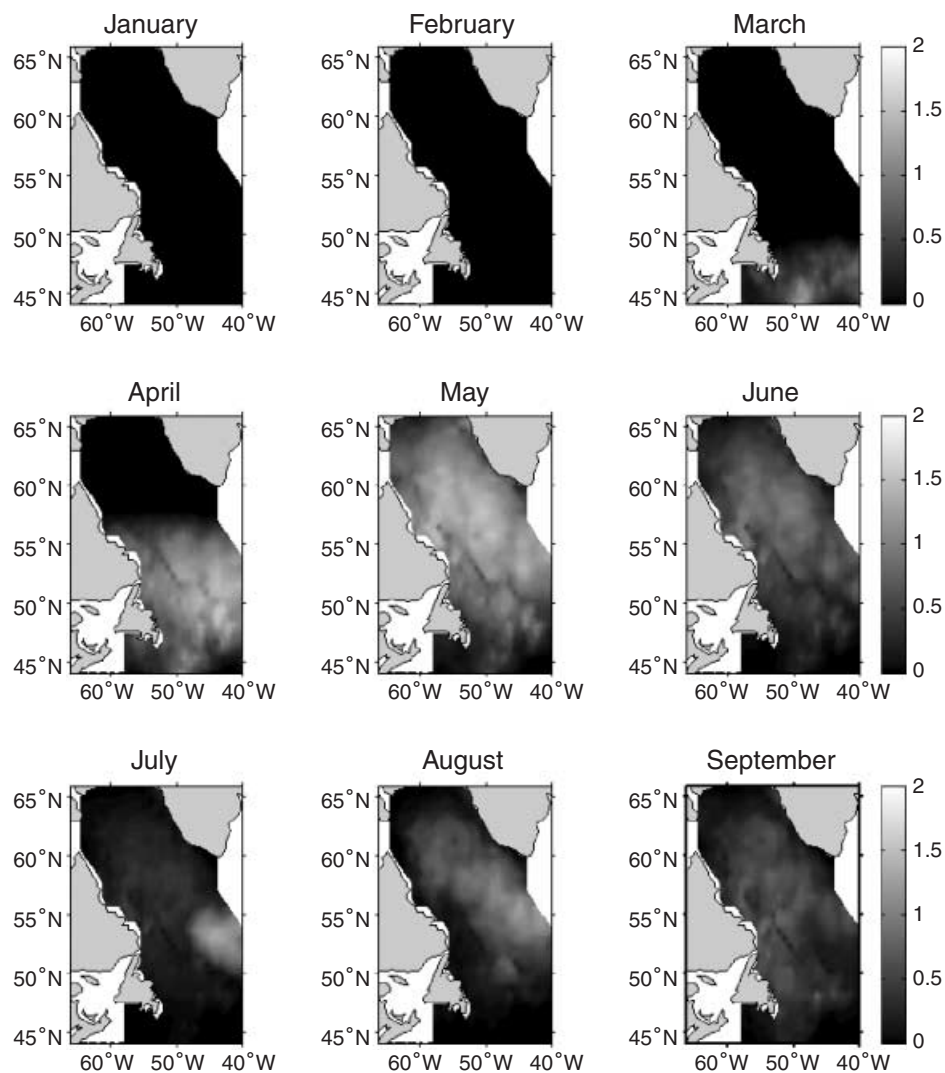


Figure 4. (a) Initial population for all runs. (b) Final population, run 1. (c) Final population, run 2. (d) Final population, run 3. $\text{Log}_{10}(x + 1)$ where x is the total number of diapausing individuals.

Run no.	Diapausing CVs, expressed as a percentage of the initial value	Percentage of individuals in diapause on day 365	Percentage of individuals to leave from eastern – northern – southern boundary
1	51.88	99.65	76.05 – 6.64 – 17.30
2	30.71	99.91	78.92 – 5.08 – 15.99
3	29.06	99.91	82.11 – 6.02 – 11.87

Table 5. Statistics for final modelled populations.

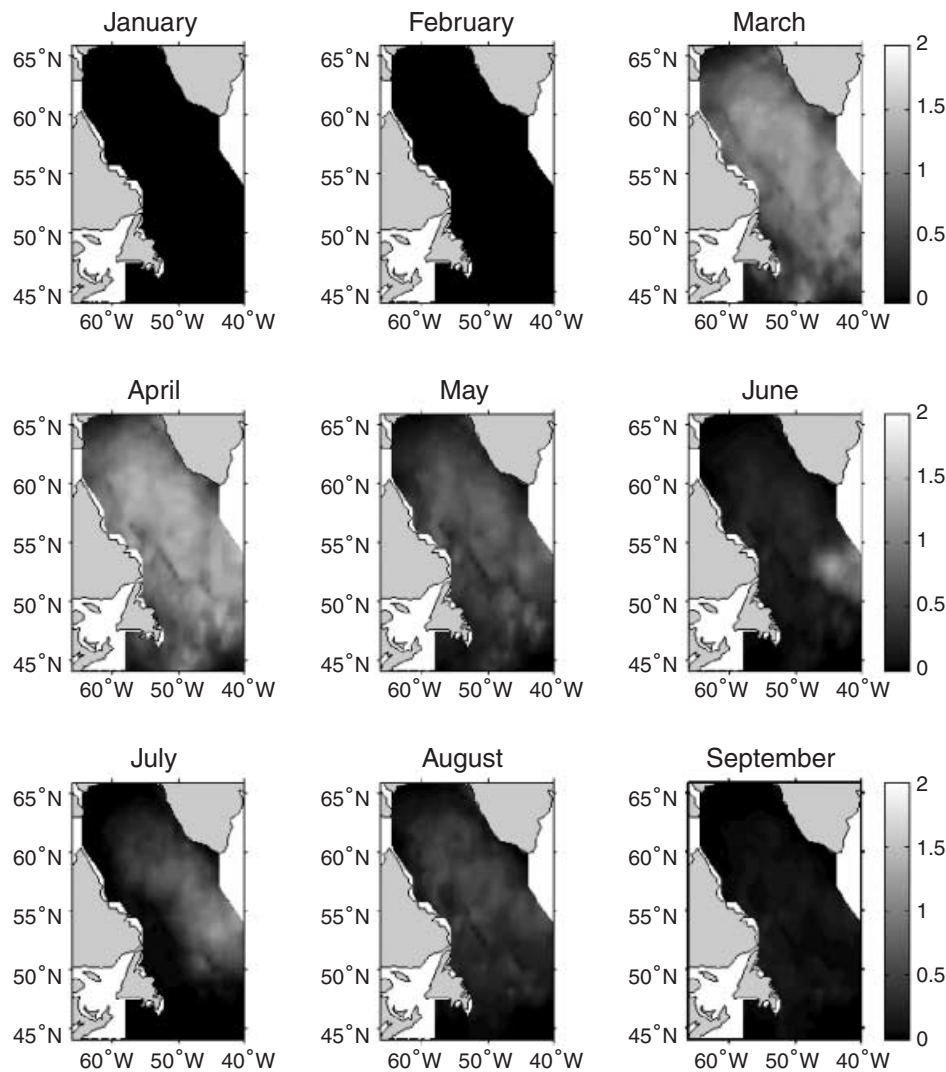
Figure 5. The results from run 1 using latitudinally dependent emergence from diapause. $\text{Log}_{10}(x + 1)$, where x is the monthly average of surface CV and adult individuals.



The final population structures of the latitudinally dependent and bi-latitudinal runs are quite similar (Fig. 4b,c). The most noticeable difference is that population numbers are a little lower (Table 5) in the bi-latitudinal run. The development of the surface

population is very different (Figs 6 and 7) in runs 2 and 3. Simultaneous emergence from diapause over the entire region can clearly be seen in run 2, with the number of individuals present at the surface peaking in March/April, and declining to near emptiness by

Figure 6. The results from run 2 using simultaneous emergence from diapause. $\text{Log}_{10}(x + 1)$, where x is the monthly average of surface CV and adult individuals.



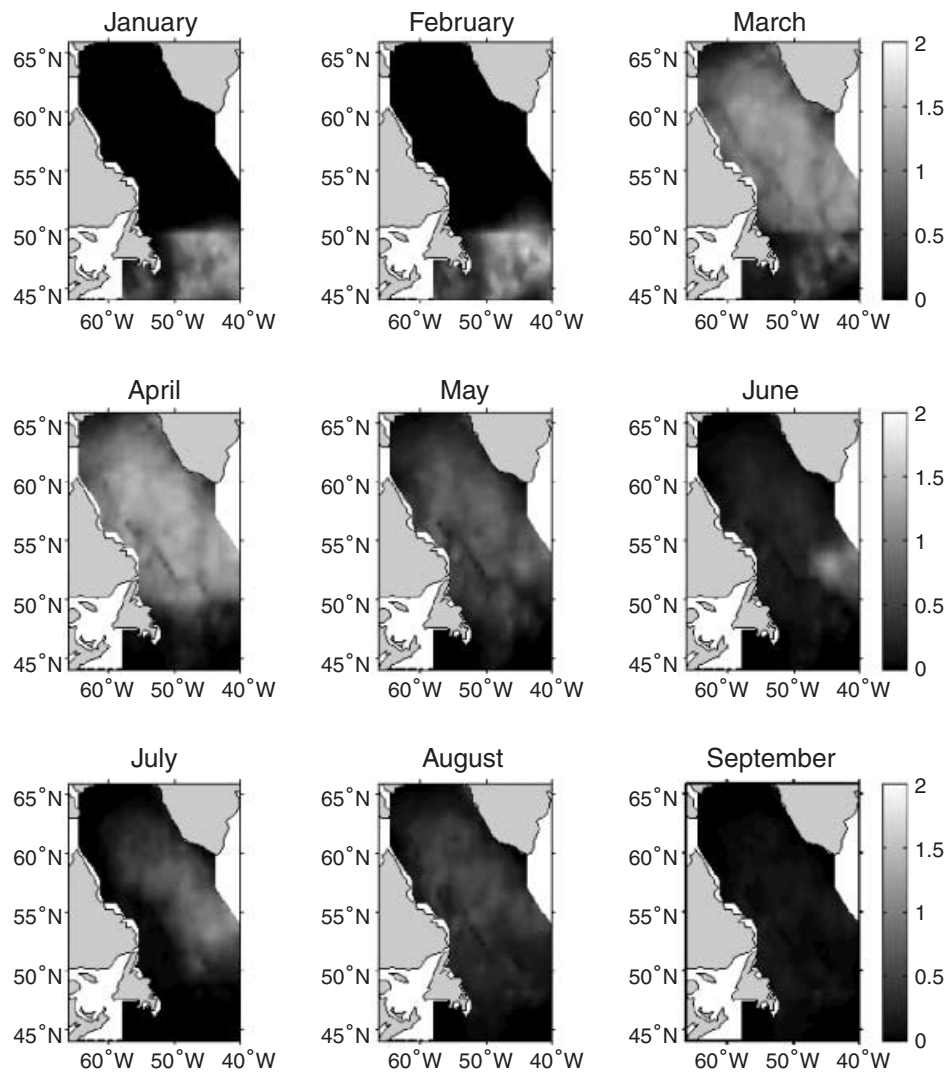
September, earlier than run 1 in both emergence and descent. Run 3 has clear surface activity to the east and south of Newfoundland in January and February, but these regions are almost devoid of activity from July until December. Activity to the north of this is almost identical to run 2.

The exit statistics from the region show that the greatest proportion of individuals leave from the eastern boundary in all model runs. On the eastern boundary, there is potential for inflows and outflows depending on the depth and the seasonal timing. This area may also be important for inward flux of individuals due to the hypothesized North Atlantic gyre structure (Head *et al.*, 2001; Tittensor, 2002).

The population in the model, as presently parameterized, decreases by around 50–70% after 1 yr, depending upon the diapause parameterization (Table 5). Although the population is tuned to near-stability in several locations from the one-dimensional run many regions will not have the same level of food availability and high ambient temperature, and we would thus expect a net population decrease in these regions.

We explored the temperature dependence of the model by carrying out runs with the mean temperature in the domain warmer or colder by as much as 1°C. Such changes in temperature have been observed over the past 40 yr in the North-west

Figure 7. The results from run 3 using bi-latitudinal emergence from diapause. $\text{Log}_{10}(x + 1)$, where x is the monthly average of surface CV and adult individuals.

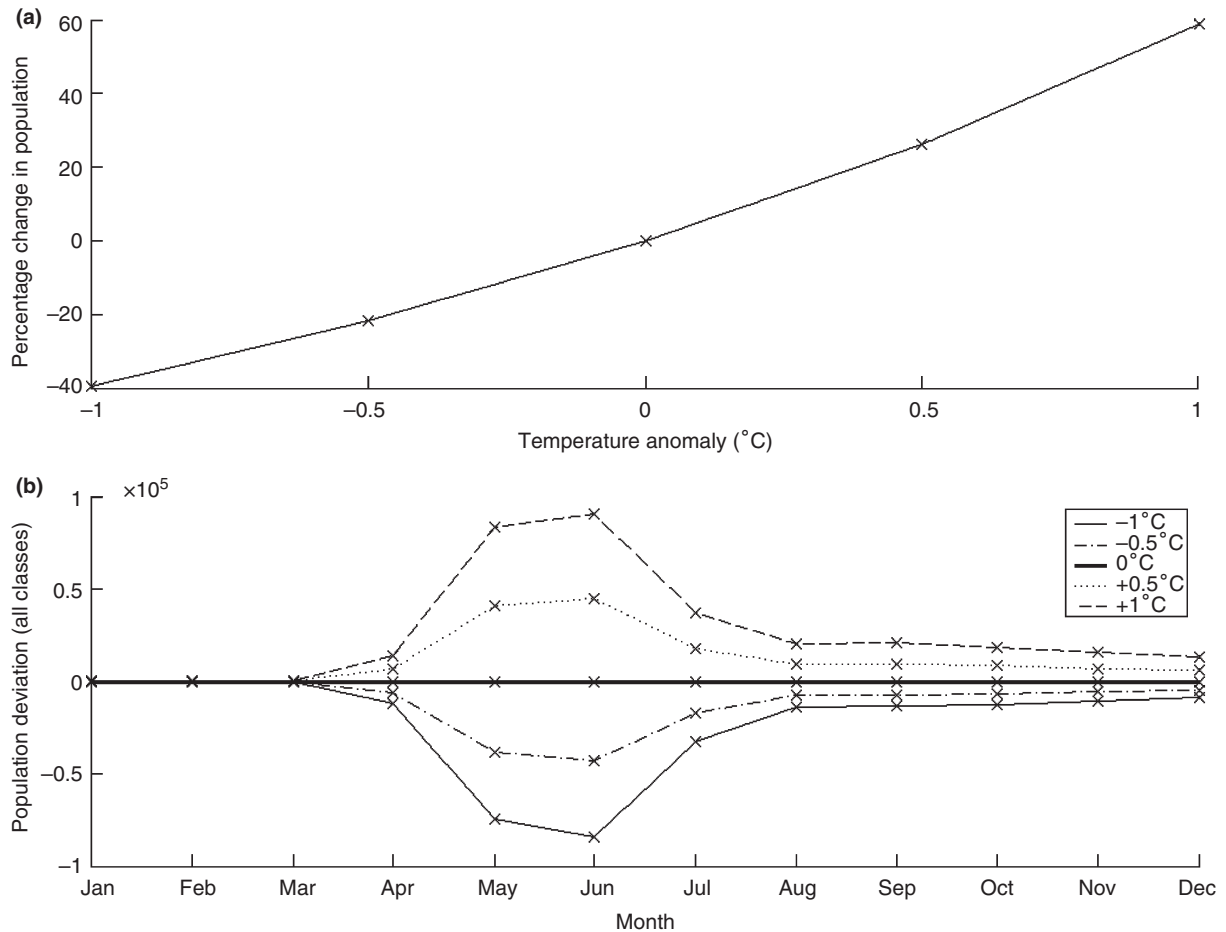


Atlantic (Dickson *et al.*, 1988) and are generally associated with changes in the North Atlantic circulation related to the North Atlantic Oscillation index. Changes in population productivity were substantial for such small changes in temperature with an increase in abundance in the model domain of 30% for 0.5°C and a decrease of 20% for a decrease of 0.5°C (Fig. 8). It can be seen from monthly anomaly plots (Fig. 8b) that most of the changes in population take place during the summer. Increases in temperature at high latitudes, where the summer surface temperature is relatively low, permit the *Calanus* to achieve greater productivity.

DISCUSSION

The spatial distributions from the model runs (e.g. Fig. 5) permit easy comparison with the observed distribution patterns from the CPR data (Fig. 1) that have been studied by Planque (1997). Our model does reproduce the key feature of the data, a surface maximum of adult *C. finmarchicus* in July/August in the middle of the Labrador Sea. Aspects of the diapause timing are not resolved in this model. Several different diapause hypotheses, simultaneous, latitudinally dependent and bi-latitudinal, all work, to varying degrees, in the model.

Figure 8. Effect of temperature on population development for the Labrador Sea population. The temperature anomaly is applied to the entire water mass in the model domain. (a) Percentage change in population after 1 yr with a constant temperature anomaly. (b) Effect of a constant temperature anomaly on population size. Values are deviations from run 1 at the end of each month. All runs based on the latitudinal diapause emergence scheme.



Run 1 does not match the timing of Matthews (1968) and Miller *et al.* (1991) particularly well, with emergence from diapause being too late in all regions except those at the same latitude as the Flemish Cap (Fig. 5). The simultaneous emergence scheme, run 2, matches somewhat poorly with Planque's data; emergence is too late to the south of Newfoundland, and too early in the north (Fig. 6). The numbers of CVs and adults peak too early. Run 3 is a slightly better fit to the data, with earlier emergence in the southern regions, and March–May being the months with most CVs and adults present at the surface (Fig. 7). This is somewhat early, but there is little activity in northern regions from October to February, which is similar to Planque's (1997) data. Run 3 matches well with the emergence timing in Matthews (1968) and hypothesized in Head *et al.* (2000) with emergence occurring earlier,

in general, than run 1, and especially so to the south and east of Newfoundland.

The production of a second generation within the area covered by the three-dimensional model is a matter of some debate; there appears to be no or little second generation in the Labrador Sea (Kielhorn, 1952; Head *et al.*, 2000), although copepodites are found at the surface during late autumn and early winter (Huntley *et al.*, 1983). Davis (1982) found at least three generations per year along the east coast of Newfoundland. Below the southern extent of the model region, off Nova Scotia, there are two generations per year in some regions (McLaren & Corkett, 1986), although once more the second may contribute little in annual production. It thus seems reasonable to assume that if a second generation did appear within the modelled region, its effects on annual productivity would be low. Model output matches Kielhorn (1952)

and Head *et al.* (2000) well, with no second generation, and copepodites that appear at the surface during the winter months appear to be slow-developing or late-spawned G1s rather than G2 individuals.

Timing of *C. finmarchicus* activity in the Labrador Sea is reproduced best with the latitudinally dependant emergence (hypothesis 1), except south of 50°N where the bi-latitudinal scheme (hypothesis 2) appears to provide a better fit when compared with Planque (1997), due to the earlier emergence of individuals to the south and east of Newfoundland. In comparison with Matthews (1968), Miller *et al.* (1991) and Head *et al.* (2000), the bilatitudinal emergence scheme produces the best results. Advective properties function essentially similarly within the separate emergence schemes, and differences in productivity occur from variance in the match or mismatch of emergence timing to warm waters and food availability.

Model run 1 is probably the most productive because the individuals emerge later relative to the other standard runs, and thus encounter warmer water, while matching the timing of the spring bloom in many regions. The model runs are all underproductive (Table 5), leading to a reduced population of diapausing individuals at the end of 1 yr. Model runs without diffusive processes are in fact more productive in all cases, although similar numbers of individuals exit the region in all runs (Tittensor, 2002). The net effect of diffusion, therefore, seems to be that more individuals are located in areas that are less suitable for growth and development (due to low temperature and/or food availability). This is borne out by visual comparison of runs with and without diffusion; more individuals are present in the low productivity north and eastern regions in the runs with diffusion. Run 1 with no diffusion and slightly reduced mortality is over-productive, as are runs with advection switched off. Thus different parameterizations would likely lead to a self-sustaining population in the Labrador Sea, and sustainability results should be interpreted with care.

Most individuals that leave the region are from the G1 generation, and exit from the eastern boundary. Individuals in the central and northern Labrador Sea have a much longer residence time than those in the south-east of the region.

Within all the standard model runs, individuals are present on most shelf and slope regions at the end of the annual cycle (e.g. Fig. 4b), areas that were not 'seeded' at the start of the year. Dispersal to these regions occurs mainly during the spring/summer with the G1 generation, as the surface currents carry the *Calanus* from the open ocean onto the shelf. Although *C. finmarchicus* overwinter in the open ocean, they are

transported onto the food-rich shelf regions by rising to the mixed layer. Utilization of surface currents may therefore place the G1 generation into a more food-rich environment.

The model population of *Calanus* is remarkably sensitive to temperature, showing changes in abundance that are as much as 20–30% over an annual cycle for a half degree change in temperature. Such changes in temperature have indeed been observed in this region over this period and their effects on fish populations discussed (deYoung and Rose, 1993). There is no evidence from the CPR data (Planque, 1997) that *Calanus* have declined in the Labrador Sea from the 1960s to the 1990s, during a time when the mean surface temperature has shown decadal variability of this amplitude, although there is evidence of dramatic changes in the north-east Atlantic (Edwards *et al.*, 2002). The temperature sensitivity of the population raises interesting questions that cannot be answered with this modelling study.

In conclusion, the model fits well with observed spatial and temporal activity patterns from the CPR survey (Planque, 1997) with a mixture of hypothesis 1, latitudinal diapause, and hypothesis 2, bi-latitudinal diapause; a latitudinally dependent emergence scheme for central and northern parts of the region, but earlier emergence to the south of Newfoundland. Other diapause emergence models are, however, also possible. The fit to the CPR survey (Planque, 1997) is reduced when using an emergence scheme derived from hypothesis 2, as is the match to the timing of the spring bloom. It would therefore seem that there is some variability in the emergence timing of individuals over the region. The contradictions of data on emergence timing for the region are difficult to resolve. Using a diapause emergence scheme based on observational evidence (run 1, Kielhorn, 1952; Anderson, 1990), individuals emerge immediately prior to the bloom in most locations. Utilizing a diapause emergence scheme based upon bilatitudinal emergence (Matthews, 1968; Miller *et al.*, 1991; Planque, 1997) decreases the match between emergence timing and the spring bloom. The bloom occurs later in more northerly regions (Fig. 2) in the SeaWiFS data, in contrast to the data from the cruises of Head *et al.* (2000). A latitudinally dependent emergence scheme with later emergence in the north thus provides surface individuals with more food and warmer waters.

ACKNOWLEDGEMENTS

This work would not have been possible without valuable input from a number of people. In particular,

the authors wish to thank G. Harrison for generating SeaWiFS data boxes at short notice, P. Pepin for suggesting use of the SeaWiFS data, G. Evans for a number of useful comments on early results of this work, P. Trela for advice regarding the biological model, and B. DeTracey for advice on the physical model. This paper arose from a masters thesis by D.P.T., financial support for which was provided by a grant to BdeY from NSERC and Memorial University of Newfoundland.

REFERENCES

- Aiken, J., Moore, G.F., Clark, D.K. and Trees, C.C. (1995) The SeaWiFS CZCS-type pigment algorithm. In: *NASA Tech. Memo. 104566*, Vol. 29. S.B. Hooker and E.R. Firestone (eds) Greenbelt: NASA Goddard Space Flight Center, 34 pp.
- Anderson, J.T. (1990) Seasonal development of invertebrate zooplankton on Flemish Cap. *Mar. Ecol. Prog. Ser.* **67**:127–140.
- Backhaus, J.O., Harms, I.H., Krause, M. and Heath, M.R. (1994) An hypothesis concerning the space-time succession of *Calanus finmarchicus* in the northern North Sea. *ICES J. Mar. Sci.* **51**:169–180.
- Blumberg, A.F. and Mellor, G.L. (1987) A description of a three-dimensional coastal ocean circulation model. In: *Three-Dimensional Coastal Ocean Models*. N.S. Heaps (ed.) Washington, DC: American Geophysical Union, **4**:1–16.
- Bryant, A., Heath, M., Gurney, W., Bearer, D.J. and Robertson, W. (1997) The seasonal dynamics of *Calanus finmarchicus*: development of a three-dimensional structured population model and application to the northern North Sea. *Neth. J. Sea Res.* **38**:361–379.
- Carlotti, F. and Radach, G. (1996) Seasonal dynamics of phytoplankton and *Calanus finmarchicus* in the North Sea as revealed by a coupled one-dimensional model. *Limnol. Oceanogr.* **41**:522–539.
- Carlotti, F. and Wolf, K.-U. (1998) A Lagrangian ensemble model of *Calanus finmarchicus* coupled with a 1-D ecosystem model. *Fish. Oceanogr.* **7**:191–204.
- Carlotti, F., Krause, M. and Radach, G. (1993) Growth and development of *Calanus finmarchicus* related to the influence of temperature: experimental results and conceptual model. *Limnol. Oceanogr.* **38**:1125–1134.
- Carlotti, F., Giske, J. and Werner, F. (2000) Modeling zooplankton dynamics. In: *ICES Zooplankton Methodology Manual*. R. Harris, P. Wiebe, J. Lenz, H.R. Skjoldal and M. Huntley (eds) London: Academic Press, pp. 571–665.
- Clarke, R.A. and Gascard, J.C. (1983) The formation of Labrador Sea water. Part II: Mesoscale and smaller-scale processes. *J. Phys. Oceanogr.* **13**:1779–1797.
- Corkett, C.J., McLaren, I.A. and Sévigny, J.M. (1986) The rearing of marine copepods *Calanus finmarchicus* (Gunnerus), *C. glacialis* (Jaschnov) and *C. hyperboreus* (Kroyer) with comment on the equiproportional rule (Copepoda). *Syngonous Natl. Mus. Can.* **58**:539–546.
- Davis, C.C. (1982) A preliminary quantitative study of the zooplankton from Conception Bay, Insular Newfoundland, Canada. *Int. Revue Ges. Hydrobiol.* **67**:713–747.
- Dickson, R.R., Meincke, J., Malmberg, S.-A. and Lee, A.J. (1988) The Great salinity anomaly in the northern North Atlantic: 1968–1982. *Prog. Oceanogr.* **20**:103–151.
- Edwards, M., Beaugrand, G., Reid, P.C., Rowden, A.A. and Jones, M.B. (2002) Ocean climate anomalies and the ecology of the North Sea. *Mar. Ecol. Prog. Ser.* **239**:1–10.
- Harris, R., Wiebe, P., Lenz, J., Skjoldal, H.R. and Huntley, M. (2000) *ICES Zooplankton Methodology Manual*. London: Academic Press, xxi + 684 pp.
- Head, E.J.H., Harris, L.R. and Campbell, R.W. (2000) Investigations on the ecology of *Calanus* spp. in the Labrador Sea. I. Relationship between the phytoplankton bloom and reproduction and development of *Calanus finmarchicus* in spring. *Mar. Ecol. Prog. Ser.* **193**:53–73.
- Head, E.H., Pepin, P. and Runge, J. (2001) Proceedings of the workshop on 'The Northwest Atlantic ecosystem – a basin scale approach'. *CSAS Proceedings Series 2001/23*. 112 pp.
- Heath, M.R. and Jónasdóttir, S.H. (1999) Distribution and abundance of overwintering *Calanus finmarchicus* in the Faroe-Shetland Channel. *Fish. Oceanogr.* **8** (Suppl. 1):40–60.
- Heath, M., Robertson, W., Mardaljevic, J. and Gurney, W.S.G. (1997) Modelling the population dynamics of *Calanus* in the Fair Isle Current off northern Scotland. *J. Sea Res.* **38**:381–412.
- Heath, M.R., Fraser, J.G., Gislason, A., Hay, S.J., Jonasdottir, S.H. and Richardson, K. (2000) Winter distribution of *Calanus finmarchicus* in the Northeast Atlantic. *ICES J. Mar. Sci.* **57**:1628–1635.
- Heath, M.R., Carlotti, F., deYoung, B., Fiksen, O. and Werner, F. (2001) *Secondary Production in the Oceans and the Response to Climate Change*. Global Change Open Science Meeting, International Geospheres and Biospheres Program, Amsterdam.
- Hirche, H.-J. (1996) Diapause in the marine copepod *Calanus finmarchicus* – a review. *Ophelia* **44**:129–143.
- Hooker, S.B. and McLain, C.R. (2000) The calibration and validation of SeaWiFS data. *Prog. Oceanogr.* **45**:427–465.
- Hooker, S.B., Esaias, W.E., Feldman, G.C., Gregg, W.W. and McClain, C.R. (1992) An overview of SeaWiFS and ocean color. *NASA Tech. Memo. 104566*, Vol. 1. S.B. Hooker and E.R. Firestone (eds) Greenbelt: NASA Goddard Space Flight Center, 24 pp.
- Huntley, M., Strong, K.W. and Dengler, A.T. (1983) Dynamics and community structure of zooplankton in the Davis Strait and Northern Labrador Sea. *Arctic* **36**:143–161.
- ICNAF (International Commission for the Northwest Atlantic Fisheries) (1963) *Environmental Surveys – NORWESTLANT 1-3, 1963* (1968) Special Publication No. 7. Nova Scotia: ICNAF.
- Ingvarsdottir, A., Houlihan, D.F., Heath, M.R. and Hay, S.J. (1999) Seasonal changes in respiration rates of copepodite stage V *Calanus finmarchicus* (Gunnerus). *Fish. Oceanogr.* **8** (Suppl. 1):73–83.
- Irigoiien, X., Harris, R.P., Head, R.N., Lindley, J.A. and Harbour, D. (2000) Physiology and population structure of *Calanus finmarchicus* (Copepoda: Calanoida) during a Lagrangian tracer release experiment in the North Atlantic. *J. Plankton Res.* **22**:205–221.
- Kalnay, E., Kanamitsu, M., Kistler, R. et al. (1996). The NCEP/NCAR 40-year reanalysis project. *Bull. Am. Meteor. Soc.* **76**:437–471.

- Kielhorn, W.V. (1952) The biology of the surface zone zooplankton of a boreo-arctic Atlantic Ocean area. *J. Fish. Res. Bd. Can.* **9**:223–264.
- Lazier, J.R.N. (1980) Oceanographic conditions at ocean weather ship Bravo, 1964–1974. *Atmos. Ocean.* **18**:227–238.
- Lazier, J.R.N. and Wright, D.G. (1993) Annual velocity variations in the Labrador Current. *J. Phys. Oceanogr.* **23**:659–678.
- Lynch, D.R., Gentleman, W.C., McGillicuddy D. Jr and Davis, C.S. (1998) Biological/physical simulations of *Calanus finmarchicus* population dynamics in the Gulf of Maine. *Mar. Ecol. Prog. Ser.* **169**:189–210.
- McClain, C.R., Esaias, W.E., Barnes, W. et al. (1992): Calibration and validation plan for SeaWiFS. In: *NASA Tech. Memo. 104566*, Vol. 3. S.B. Hooker and E.R. Firestone (eds) Greenbelt: NASA Goddard Space Flight Center, 41 pp.
- McLaren, I.A. (1986) Is structural growth of *Calanus* potentially exponential? *Limnol. Oceanogr.* **31**:1342–1346.
- McLaren, I.A. and Corbett, C.J. (1986) Life cycles and production of two copepods on the Scotian Shelf, Eastern Canada. *Nat. Mus. Can. Syllageus.* **58**:362–367.
- Mann, K.H. and Lazier, J.R.N. (1996) *Dynamics of Marine Ecosystems: Biological Physical Interactions in the Oceans*. Boston: Blackwell Science, 394 pp.
- Marshall, J., Dobson, F., Moore, K. et al. (1998) The Labrador deep sea convection experiment. *Bull. Am. Met. Soc.* **79**:2033–2058.
- Matthews, J.B.L. (1968) On the acclimatization of *Calanus finmarchicus* (Crustacea, Copepoda) to different temperature conditions in the North Atlantic. *Sarsia* **34**:371–382.
- Mauchline, J. (1998) *The Biology of Calanoid Copepods*. San Diego: Academic Press, x + 709 pp.
- Mellor, G.L. (1996) *User's Guide for a Three-Dimensional Primitive Equation, Numerical Ocean Model*. Princeton, NJ: Atmos. and Oceanic Sci. Program, Princeton Univ., 35 pp.
- Miller, C.B., Cowles, T.J., Wiebe, P.H., Copley, N.J. and Grigg, H. (1991) Phenology in *Calanus finmarchicus* (Gunnerus); hypotheses about control mechanisms. *Mar. Ecol. Prog. Ser.* **72**:79–91.
- Miller, C.B., Lynch, D.R., Carlotti, F., Gentleman, W. and Lewis, C.V.W. (1998) Coupling of an individual-based population dynamics model of *Calanus finmarchicus* to a circulation model for the Georges Bank region. *Fish. Oceanogr.* **7**:219–234.
- Petrie, B. and Mason, C.S. (2000) Satellite measurements of sea surface temperature: an application to regional ocean climate. *Canadian Stock Assessment Secretariat Research Document 2000/061*, 25 pp.
- Planque, B. (1997) *Spatial and temporal fluctuations in Calanus populations sampled by the continuous plankton recorder*. PhD Thesis, Universite Pierre et Marie Curie (Paris VI), 81 pp.
- Siegel, D.A., Doney, S.C. and Yoder, J.A. (2002) The North Atlantic spring phytoplankton bloom and Sverdrup's critical depth hypothesis. *Science* **296**:730–733.
- Slagstad, D. and Tande, K.S. (1996) The importance of seasonal vertical migration in across shelf transport of *Calanus finmarchicus*. *Ophelia* **44**:189–205.
- Smith, S.D. (1988) Coefficients of sea surface wind stress, heat flux, and wind profiles as a function of wind speed and temperature. *J. Geophys. Res.* **93**:15467–15472.
- Smith, S.D. and Dobson, F.W. (1984) The heat budget at Ocean Weather Station Bravo. *Atmos. Ocean* **22**:1–22.
- Tang, C.L. and Wang, C.K. (1996) A gridded data set of temperature and salinity for the Northwest Atlantic ocean. *Can. Data Rep. Hydrogr. Ocean. Sci.* **148**:1–45.
- Tittensor, D.P. (2002) *Population distributions of the copepod Calanus finmarchicus in the Labrador Sea: a modelling study*. MSc Thesis, Memorial University of Newfoundland, xvii + 192 pp.
- Trela, P. (1996) *Effect of spatial and temporal variability in oceanic processes on air-sea fluxes of carbon dioxide*. PhD Thesis, Dalhousie University, Halifax, xvii + 221 pp.
- Woods, J.D. and Barkmann, W. (1993) Diatom demography in winter, simulated by the Lagrangian method. *Fish. Oceanogr.* **2**:202–222.
- Yao, T., Tang, C.L. and Peterson, I.K. (2000) Modeling the seasonal variation of sea ice in the Labrador Sea with a coupled multicategory ice model and the Princeton Ocean model. *J. Geophys. Res.* **105**:1153–1165.
- deYoung, B. and Rose, G. (1993) On recruitment and distribution of Atlantic cod (*Gadus morhua*) off Newfoundland. *Can. J. Fish. Aquat. Sci.* **50**:2729–2741.